Crack-healing in crosslinked styrene–co-acrylonitrile

T. Q. Nguyen, H. H. Kausch, K. Jud and M. Dettenmaier
Laboratoire de Polymères, Ecole Polytechnique Federale de Lausanne, 1007 *Lausanne, Switzerland*
(*Received* 2 *June* 1981; *revised* 28 *September* 1981)

The crack-heating behaviour of γ-irradiated poly(styrene-co-acrylonitrile) (SAN) was investigated as a function of radiation dose over the range 0–800 Mrad. The predominant response of SAN to γ-irradiation is crosslinking as evidenced by the radiation yields G_x (crosslink) = 0.077 and G_s (main chain scission) = 0.055. The presence of crosslinks considerably increased the time required for complete reheal of compact tension (CT) specimens. Fracture mechanics testing on non-irradiated samples showed that the energy release rate, G_I, increased linearly with the square root of the rehealing time, t_p, until the original value of the energy release rate, G_{Io}, of the virgin material was restored. In contrast, for crosslinked samples, the initial increase in energy release rate, G_I, was followed by a plateau region at a value of G_{Ip} which was less than G_{Io}. A further recovery was observed over a long time scale, some minutes to one hour after the first plateau (G_{Ip}) was reached. The ratio of the plateau value and the original fracture toughness (G_{Ip}/G_{Io}) was found to vary with the square root of the average molecular weight between cross-links, $\bar{M}_x$. This phenomenon may be correctly explained in terms of the average length of free chains formed during the fracture process. A simple double-layer diffusion model describes well the existence of the two recovery regions, it is not yet sufficient, however, since the form of the transition from the first to the second recovery mechanism is not adequately represented by this model.

Keywords Crack-healing; fracture mechanics; gamma irradiation; diffusion; styrene–acrylonitrile copolymer; thermoplastics

INTRODUCTION

Kausch and collaborators[1-7] have previously reported that crack-healing of amorphous polymers slightly above T_g involves the diffusion of macromolecules across the interface. Their fracture mechanics experiments have clearly shown that there is a linear proportionality between the fracture energy, G_{Ii}, of the rehealed crack zone and the square root of the rehealing time, t_p. It was also possible to explain the observed time- and temperature-dependence of G_{Ii} by a diffusion model of entanglement formation[2-7]. An analysis of the microscopic deformation process at the crack tip shows[7-8] that the energy of deformation, i.e. G_{Ii}, depends linearly on the number, n, of entanglements formed at the interface:

$$G_{Ii}(t_p, T_p) = \beta n(t_p, T_p) \tag{1}$$

where T_p is the temperature at which healing was achieved. The constant β can be derived from the 'completely healed' state with n_0 entanglements per unit fracture surface area:

$$\beta = G_{I0}/n_0 \tag{2}$$

It was further assumed that $n(t_p)$ is built up by a diffusion process:

$$\frac{n(t_p)}{n_0} = \frac{(2Dt_p)^{\frac{1}{2}}}{(\langle y^2 \rangle)^{\frac{1}{2}}} \tag{3}$$

where $(\langle y^2 \rangle)^{\frac{1}{2}}$ is the average depth of interpenetration to be achieved by the molecules in order to form n_0 entanglements, and D is their diffusion coefficient. Equations (1) and (3) do not permit determination of D and $\langle y^2 \rangle$ independently.

In order to obtain additional information on the nature of the diffusion mechanism it was decided to study the crack-healing in crosslinked polymers. The results of this work turned out to be rather unexpected. Since their interpretation depends strongly on a thorough understanding of the network structure of the crosslinked samples some effort has been placed on network characterization.

EXPERIMENTAL

Compact tension (CT) specimens were compression moulded from granules of styrene–acrylonitrile copolymer (SAN) after careful drying *in vacuo* to remove any adsorbed water. The granules were provided by BASF and are marketed under the trade name LURAN 368R. The acrylonitrile content is 38 mol per cent as determined by elementary analysis which corresponds to the azeotropic composition for this copolymer. To crosslink the samples, unbroken CT specimens, $26 \times 26 \times 3$ mm^3 in size, were irradiated with γ-rays at room temperature in vacuum-sealed Pyrex tubes to a predetermined dose up to 800 Mrad (Sulzer source of ^{60}Co of 50 kCi). SAN belongs to the group of polymers which mainly undergo crosslinking during irradiation[10].

0032-3861/82/091305-06$03.00

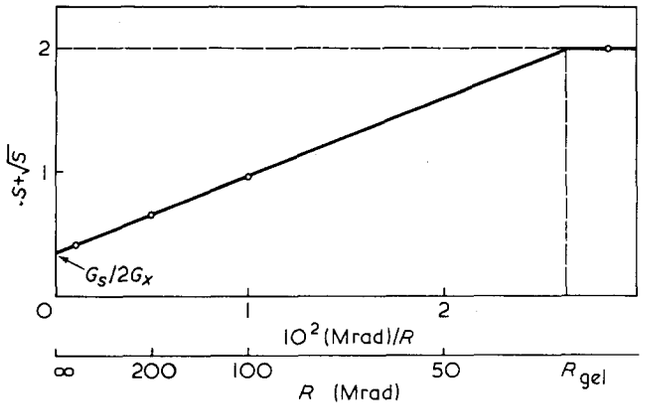

Figure 1 Charlesby–Pinner plot of irradiated Luran(R) 368 R (solubility of irradiated SAN)

It is well known that reactive species, ions and free radicals, are still present in appreciable amounts after irradiation in polymeric materials[11]. In order to eliminate any post-irradiation effect, all the samples were annealed under vacuum, before measurements, for several days at a temperature T_{irr} some 5K above the glass transition temperature, T_g. The irradiated and annealed CT specimens were subsequently broken at room temperature and submitted to a rehealing treatment as described before[1].

Characterization of the crosslinked network

In order to give a quantitative interpretation to the rehealing experiments, the polymer network must be well characterized with particular attention on the average distance between two crosslinking points.

In our laboratory, molecular weight measurements on non-irradiated samples gave an $\bar{M}_n$ of 100000 by osmometry and an $\bar{M}_v$ of 160000 by viscosimetry. An evaluation of our gel permeation chromatography measurements, based on the universal calibration curve[12], confirmed that the molecular weight distribution is close to the random distribution with an $\bar{M}_w$ of 230000.

The characteristic parameters of the irradiated network can be derived from the gel fraction g following the evaluation of Charlesby[13]. Therefore, the gel fraction g of irradiated samples was determined by Sohxlet extraction with boiling tetrahydrofuran for 72 h under a nitrogen atmosphere. The residue was dried to constant weight in vacuum at a temperature slightly above T_g. The sol fraction s was obtained by subtraction as $s=1-g$.

For an initially random molecular weight distribution, $s+\sqrt{s}$ is inversely proportional to the irradiation dose R according to the relation[13]:

$$s+\sqrt{s}=(R_{gel}/R)(2-G_s/2G_x)+G_s/2G_x \qquad (4)$$

where R_{gel} is the dose for gel formation, and G_s and G_x are the yields for chain scission and crosslinking respectively.

The plot of $s+\sqrt{s}$ as a function of $1/R$, shown in *Figure 1*, gives a straight line thus corroborating the g.p.c. results which intimate that the molecular weight of the original sample follows a random distribution[13].

The dose R_{gel} is determined from the sol curve (*Figure 1*) at $s+\sqrt{s}=2$, where it is equal to 38 Mrad. Extrapolation towards infinite dose gives a value of 0.36 for the ratio $G_s/2G_x$. In pure polystyrene, $G_s/2G_x$ is 0.03[14]. The higher ratio that we found for the copolymer may be explained by the presence of acrylonitrile in the monomer sequence since main chain scission is more prevalent in γ-irradiated polyacrylonitrile[15]. With the dose expressed in Mrad, the radiolytic yield for crosslinking, G_x, is given by the following expression[13]:

$$4G_x-G_s=\frac{0.96\cdot10^6}{R_{gel}\cdot\bar{M}_n} \qquad (5)$$

The value of 0.077 thus derived for G_x is slightly larger than the G_x of 0.047 found in polystyrene[14].

The next step of the evaluation is the determination of $\bar{M}_x$, the number average molecular weight of a chain segment containing one crosslinked unit. In highly crosslinked samples $\bar{M}_x$ corresponds to the average length of a segment between adjacent crosslinking points. Due to the simultaneous occurrence of scission and crosslinking in SAN, the calculation of $\bar{M}_x$ is more complex than in a specimen which exclusively crosslinks under irradiation. Under the hypothesis that scission and crosslinking occurred at random, it is possible to separate temporarily the two effects. The two processes are considered as occurring consecutively rather than simultaneously. Firstly, chain scission modifies the *MWD* and decreases $\bar{M}_n(0)$ to $\bar{M}_n(R)$, where $\bar{M}_n(R)$ is the hypothetical number average molecular weight of the sample at a given dose R in the absence of crosslinking and $\bar{M}_n(0)=\bar{M}_{n0}$ is the initial number average molecular weight at zero dose.

The relation between $\bar{M}_n(R)$ and $\bar{M}_{n0}$ for an initially random distribution is given by[13]:

$$\frac{1}{\bar{M}_n(R)}=\frac{1}{\bar{M}_{n0}}+\frac{R\cdot G_s}{0.96\cdot10^6} \qquad (6)$$

The second step comprises crosslinking the new *MWD* obtained after completion of main chain scission. The resulting number average molecular weight $\bar{M}_x$ of chains 'between crosslinking points' is equal to $\bar{M}_n/\gamma$ where γ is the crosslinking index defined as the number of crosslinked units per number average molecule. Experimentally, γ is related[13] to the sol content by:

$$\gamma=1/(s+\sqrt{s}) \qquad (7)$$

The preceding measurements and considerations are necessary and sufficient to compute $\bar{M}_x$ as:

$$\bar{M}_x=\bar{M}_n\cdot(s+\sqrt{s}). \qquad (8)$$

Since it is important to realize that even after gel formation there is a large quantity of soluble, small crosslinked chains present, in *Figure 2* the theoretical behaviour of a monodisperse polymer sample which crosslinks exclusively under irradiation is shown. At the start of irradiation, there is no network formation but an increase in the number of branched molecules P_2, P_3, etc. After the gel point, corresponding to $\gamma=1$ for an initially monodisperse *MWD* or to $\gamma=\frac{1}{2}$ for an initially random *MWD*, the molecules with the highest molecular weights (and also with the highest degree of branching) are incorporated into the network at a faster rate than the smaller molecules. As a consequence the density of crosslinks in the gel is higher than in the sol. The value of

$\bar{M}_x$ given by equation (8) is an overall average. The true average molecular weight between two crosslinks in the gel, $\bar{M}_{xg}$, must, therefore, be corrected and is given by[13]:

$$\bar{M}_{xg} = M_x/(1+s) \tag{9}$$

The above treatment is only valid under the hypothesis of random scission and crosslinking, with G_s and G_x independent of radiation dose. Since this assumption need not be true *a priori*[16], it is advisable to measure $\bar{M}_x$ independently by some other means such as the swelling technique. The relation between $\bar{M}_{xg}$ and the swelling ratio of a gel at equilibrium is given by the Flory equation[17]:

$$\frac{1}{\bar{M}_{xg}} = \frac{2}{M_n} - \frac{(\bar{v}/V_1)[\ln(1-v_s)+v_s+\chi v_s^2]}{[v_s^{1/3}-\frac{1}{2}v_s]} \tag{10}$$

where $\bar{M}_n$ = number average molecular weight of the sample before crosslinking, given by equation (6); $\bar{v}$ = specific volume of the polymer, equal to 0.932 cm^3/g for LURAN® 368R; V_1 = molar volume of the solvent, equal to 81.94 $cm^3\ mol^{-1}$ for tetrahydrofuran; v_s = volume fraction of the polymer in the swollen sample at equilibrium; (the sol fraction is excluded from the calculation) and χ = Flory–Huggins parameter for polymer–solvent interaction equal to 0.405 for the couple LURAN® 368/THF at 30°C, determined from the second virial coefficient by osmometry.

In *Table 1*, $\bar{M}_{xg}$ as computed from equations (9) and (10) is given for different doses. In view of the experimental errors and theoretical simplifications inherent to the swelling method, the values of $\bar{M}_x$ and $\bar{M}_{xg}$ obtained from equations (8) and (9) are probably more reliable and will be used in the discussion which follows.

RESULTS OF MECHANICAL TESTS AND OBSERVATIONS

In the mechanical tests the force, P, necessary to propagate in the CT specimens a pre-existing crack of length a. From these data the fracture toughness, K_{Ii}, can be calculated as follows:

$$K_{Ii} = YP\sqrt{a}/WB \tag{11}$$

where W and B are respectively the specimen width and thickness and Y a geometrical correction factor[1]. The fracture toughness, K_{Ii}, at crack initiation was thus measured on the rehealed CT samples as a function of contact time, t_p. The samples had been exposed to various degrees of crosslinking before the fracture and rehealing treatment. As shown in *Figure 3*, an initial linear

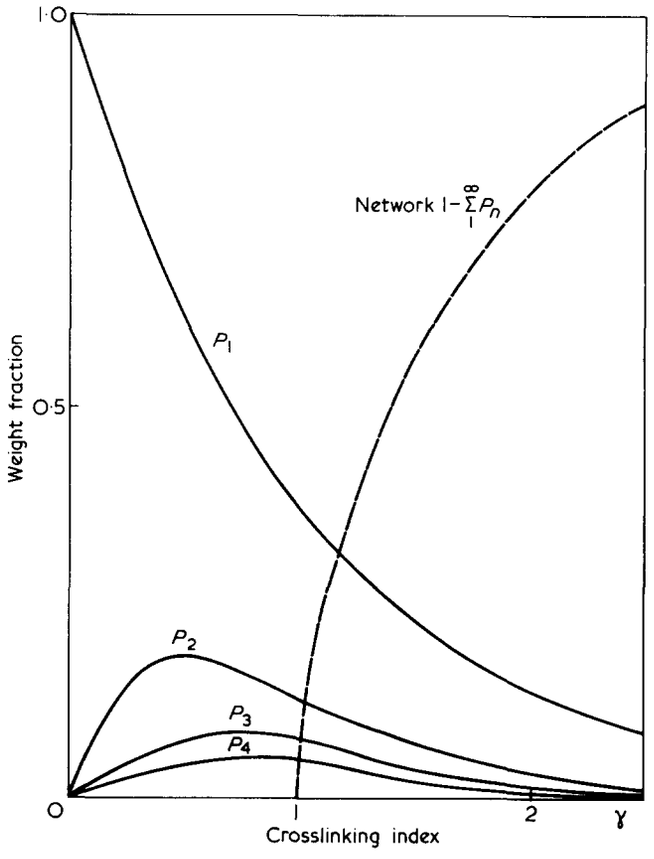

Figure 2 Crosslinking of a monodisperse polymer

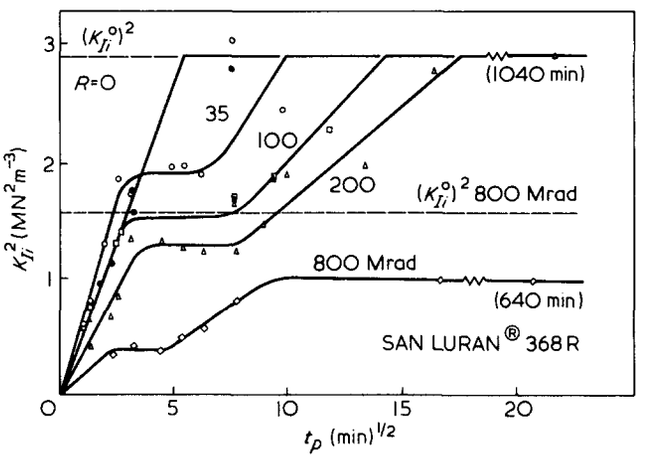

Figure 3 Fracture energy as function of rehealing time and irradiation dose: (●) = experimental points for unirradiated SAN; (○) = experimental points for SAN irradiated to 35 Mrad; (□) = experimental points for SAN irradiated to 100 Mrad; (△) = experimental points for SAN irradiated to 200 Mrad; (◇) = experimental points for SAN irradiated to 800 Mrad

Table 1 Characterization of the polymer network in crosslinked Luran 368R

Dose	% Soluble	γ	$\bar{M}_n$	$\bar{M}_x$ (from equations (6–9))	$\bar{M}_{xg}$ (from equations (6–9))	Swelling ratio of volume	$\bar{M}_{xg}$ (from equation (10))
0	100	0	100 000	–	–	–	–
35	100	0.47	83 200	–	–	–	–
100	35.2	1.02	63 400	62 100	45 900	29.9	28 000
200	20.6	1.49	46 400	31 200	25 800	16.9	18 100
800	11.9	2.29	17 800	7800	6980	8.09	6000

Table 2 Relationship between value of the plateau energy and $\bar{M}_x$

Dose (Mrad)	$\sqrt{\frac{1}{2}\bar{M}_x}$	$\sqrt{\bar{M}_x/200\,000}$	K^2_{Ip}/K^2_{Io}
0	–	–	1
35	203	0.64	0.65
100	176	0.56	0.52
200	125	0.40	0.45
800	62	0.20	0.25

dependence between the square of K_{Ii} and $t_p^{1/2}$ is observed both with crosslinked samples and non-irradiated samples. The linear increase of K_{Ii}^2 is followed by a plateau region (K_{Ip}^2). However, whereas K_{Ii}^2 of an uncrosslinked sample reaches a plateau value only when the original fracture toughness K_{Ip}^2 is fully restored, the irradiated samples show a plateau at a value K_{Ip}^2 smaller than K_{Io}^2 (*Figure 3*). The plateau value decreases with the dose received and there is a good correlation between K_{Ip}^2/K_{Io}^2 and the square root of $\bar{M}_x$ (*Table 2*).

Another striking fact in irradiated samples is the occurrence of a second recovery in fracture toughness which began some minutes to one hour after the first plateau was reached. With the exception of the highest dose of 800 Mrad, the original fracture toughness of the virgin material was eventually restored. The second recovery gives a straight line on a K_{Ii}^2 vs. $t_p^{1/2}$ plot, suggesting that a diffusion process is also responsible for this stage. The modest variation of the slopes for the initial recovery of fracture energy for all samples, regardless of the irradiation dose, indicates that crosslinkage before fracture influences little the kinetics of the first stage of rehealing.

DISCUSSION

Specimens which had received a dose of 200 Mrad after fracture did not show any measurable rehealing at 390 K, even after several days of penetration. The creation of a fracture surface seems to be necessary, therefore, before healing can occur in crosslinked samples. It is known that the superficial layer next to the fracture surface is highly affected by the fracture process resulting in disentanglements of molecular coils and chain scissions. In highly crosslinked polymers, chain scission will be prevalent, a fact which has been well documented in the past using e.s.r. spectroscopy[18]. The net effect in the used samples may well be the formation of two layers: a first layer (region A in *Figure 4*) which consists essentially of free chain ends liberated by slippage from the matrix or created by breakage of segments between crosslinking points. The width of this layer can be estimated to be given by $(\langle R_e^2 \rangle)^{\frac{1}{2}}$ the average distance between a chain end and the nearest crosslink along the chain. Adjacent to this region A of highly mobile chain ends, one finds a region B (cf. *Figure 4*) plastically deformed by the fracture event. In order to explain the second recovery it is required that this layer B also contains mobile chains but that their degree of mobility be much smaller than that of the A-chains. The lower mobility could be ascribed, for instance, to the greater length of the diffusing units and to the presence of crosslinks in the matrix hindering the diffusion even of the uncrosslinked chains.

The two-layer model presented in *Figure 4* is certainly a simple model and its limits will become apparent in the later discussions. We will at first attempt to relate the value of K_{Ip}^2 with the width a of the highly mobile region A.

Magnitude of K_{Ip}^2

It is evident that only chains with their ends within a certain distance of the interface can diffuse easily across this interface and give effective contributions to the transmission of mechanical stress[1-7,19]. In the present case a chain segment of molecular weight M_1 may be considered, which is attached to a crosslink point at a distance d_1 from the interface. If d_1 is no greater than the radius of gyration, R_{g1}, then the end of this particular segment has a good chance of crossing the interface. The width a of region A in *Figure 4* should be taken, therefore, as the radius of gyration of the free chain segments found in region A. No matter whether those chain segments are liberated by slippage or created by breakage, they will have a number average molecular weight of $\bar{M}_x/2$. If it can be assumed that the free chain segments assume a random coil conformation then the width a of the highly mobile layer will be given by:

$$a = \sqrt{\frac{\bar{M}_x}{2}} \cdot \left\langle \frac{R_g^2}{M} \right\rangle_0^{\frac{1}{2}} \tag{12}$$

For the molecular-weight independent term $\left\langle \frac{R_g^2}{M} \right\rangle_0^{\frac{1}{2}}$ we may take the value of $7 \cdot 10^{-4}$[nm²·mol/g] determined by Kirste *et al.*[20]. During the healing treatment a fracture energy $G_{Ii} \sim K_{Ii}^2$ will be built up, first by interdiffusion of the mobile segments analogous to our observations with uncrosslinked polymers[1-7,9]; K_{Ii}^2 is, therefore, proportional to the distance of interpenetration. Once this distance has reached the value of a, the chain ends are completely interdiffused. At this moment we have:

$$K_{Ip}^2/K_{Io}^2 = a/a_0$$

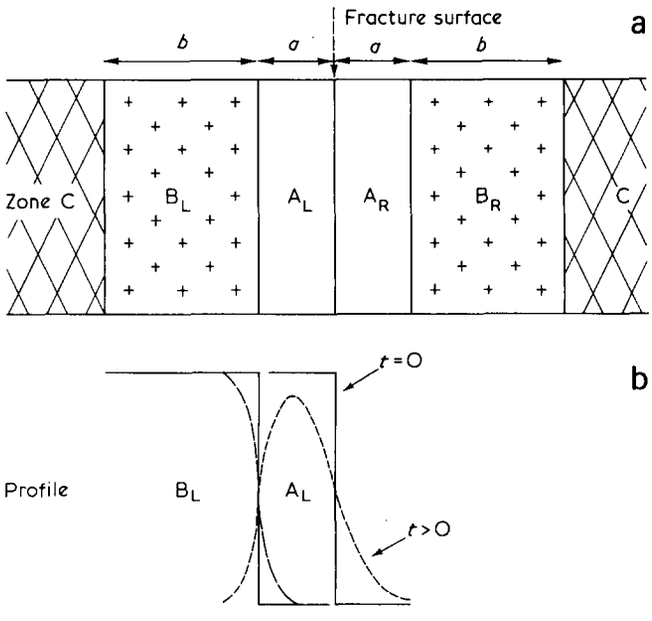

Figure 4 Model of two-layer interdiffusion: (a) = geometric representation of the diffusion layers; (b) = concentration profile of the diffusing species at two different times

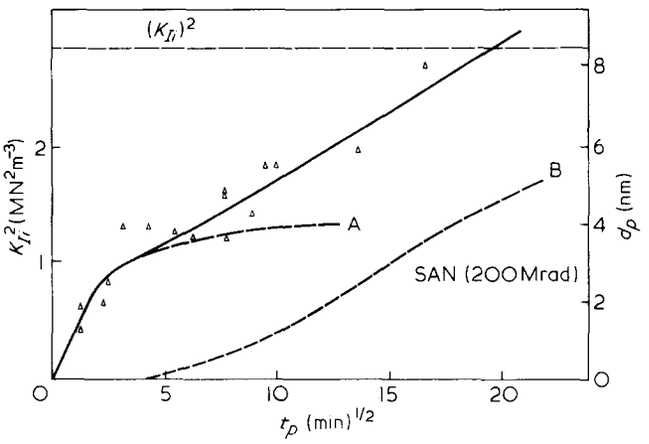

Figure 5 Comparison of fracture energy with theoretical two-mechanism diffusion curve. The parameters used for the calculations are: $D_A = 4.3 \cdot 10^{-21}$ m^2.s^{-1}; $D_B = 0.36 \cdot 10^{-21}$ m^2.s^{-1}; $a = 4 \cdot 10^{-9}$ m; $b = 8 \cdot 10^{-9}$ m. Curves (A) and (B) refer to diffusion of species A and B respectively. The penetration distances, d_p, on the right-hand scale are calculated with the value of $\langle R_g^2 \rangle_0 / M$ cited in the text

where a_0 is the interpenetration distance necessary to establish the full strength of the virgin material. If a_0 is taken to be the radius of gyration of an average original molecule ($\bar{M}_{n0} = 100\,000$), one should have:

$$K_{Ip}^2 / K_{Io}^2 = \sqrt{\bar{M}_x / 200\,000} \qquad (13)$$

As is revealed by *Table 2*, there is indeed a good linear correspondence between K_{Ip}^2 and $\sqrt{\bar{M}_x}$. The fact that at high degrees of crosslinking K_{Ip}^2/K_{Io}^2 is found to be slightly larger than $\sqrt{\bar{M}_x/200\,000}$ might be due to a non-random cutting of chain segments in the first fracture process and to an underestimation of $\bar{M}_x$. In view of the very wide molecular weight distribution of the original sample this aspect will not be pursued any further.

The second recovery in fracture toughness and the double layer model

If chain ends were the only diffusing species, no increase in G_I should be observed after the plateau energy G_{Ip} is reached. The occurrence of the second recovery in fracture toughness over a long time scale indicates that less mobile species, able to give rise to additional entanglements, are also present near the fracture surfaces. These may be formed from the remains of the broken network disentangled during the fracture. The presence of crosslink points considerably lowers the diffusion coefficient so that linear or very lightly branched portions of these molecules start to intermingle only after complete interdiffusion of the chain ends.

We present below (*Figure 4*) a mathematical model with two diffusing layers to reproduce the two-step diffusion process mentioned above. Symbol A represents the free chain ends which constitute the mobile layers and B the (branched) portion of the molecules forming the second layer. $\underline{a}$ and $\underline{b}$ are the thickness of each layer respectively; the suffixes L and R refer to the left and right-hand side of the broken sample.

The movements of A and B will be correlated if the two species are bound together and belong to the same molecule. However, to make the mathematics easier, we will assume that they are independent and that the diffusion of each species follows Fick's law. This need not be true for the actual system under investigation, however, the simplified model allows us to study some basic characteristics of a two-step diffusion process.

The model given above is described by two diffusion coefficients: the self-diffusion coefficient D_A of A_L into A_R, and the mutual diffusion coefficient D_B of A_L into B_R (or A_R into B_L). The number of entanglements formed is proportional to the number of species A and B which have diffused across the boundary at $x = 0$. Symmetry around the fracture plane allows us to consider only the right half of the broken sample.

$$G_I(t) \propto \int_0^{a+b} \{C_{A_L}(x,t) + C_{B_L}(x,t)\} \mathrm{d}x. \qquad (14)$$

C_{A_L} and C_{B_L} are the concentrations of A_L and B_L respectively. Analytical expressions for $C_A(x,t)$ and $C_B(x,t)$ can be obtained from standard mathematical diffusion techniques[21]. The explicit expressions are given in the Appendix. The curves shown in *Figure 5* are the results of numerical integration of C_A and C_B. The best fit to the experimental data for specimens irradiated to 200 Mrad is obtained with $D_A/D_B = 12$. This confirms the earlier speculation that the B layer, being partially crosslinked, has a much lower diffusivity than the A layer. It may be noted from *Figure 5* that the model used so far does not lead to a well pronounced plateau. We may hope that a refined model, which accounts for the orientational reorganization at the fracture surface and for an eventual coupling of molecules belonging to the two different regions, will lead to a better description of the experimental data.

CONCLUSION

Mechanical tests on rehealed crosslinked polymers reveal many interesting features which cannot be studied solely with linear macromolecules. In particular, the difference in mobility between free chain ends and chains in a crosslinked environment unveils itself in an enlightening manner as a plateau in the fracture curve. These experiments again confirm the usefulness of the rehealing technique as a powerful tool for the investigation of bulk polymer diffusion at temperatures just above T_g. At these temperatures, the rate of diffusion is so small that only the mechanical effects of the transport process can be measured, but not the diffusion distances themselves. An estimation shows that the minimum penetration depth to fully restore the original toughness of LURAN 368R is equal to 8 nm. It should be essentially independent of the molecular weight of the starting material. Experiments with fractions of SAN are underway in our laboratory to check this hypothesis.

ACKNOWLEDGEMENTS

The authors would like to thank the Institute of Physical Chemistry, EPF Lausanne, for the use of the ^{60}Co source, and Dr G. Dolivo who carried out most of the irradiations for the experiments presented in this paper. Financial support of the Swiss National Science Foundation is gratefully acknowledged.

REFERENCES

1 Jud, K. and Kausch, H. H. *Polym. Bull.* 1979, **1**, 697
2 Jud, K., Kausch, H. H. and Williams, J. G. *J. Mater. Sci.* 1981, **16**, 204
3 Jud, K. and Kausch, H. H. 'Advances in Fracture Research', Vol. II, Pergamon Press, Oxford–New York, 1981, 755
4 Kausch, H. H. Spring Meeting of the German Physical Society, Division of High Polymers, Marburg, 18–20th March 1981, *Colloid and Polymer Sci.* 1981, **259**, 917
5 Hguyen, T. Q. and Kausch, H. H. Société Suisse de Physique, Neuchâtel, 9/10 April 1981
6 Kausch, H. H. 12th Europhysics Conference on Macromolecular Physics, Leipzig, 21–26th September 1981, Europhysics Conference Abstracts, 51, 59 (1981)
7 Jud, K. *PhD Thesis*, Swiss Federal Institute of Technology, Lausanne, 1981
8 Könczöl, L., Döll, W., Kausch, H. H. and Jud, K. *Kunststoffe* 1982, **72**, 46
9 Kausch, H. H. and Jud, K. 13.Sitzung des Arbeitskreises Bruchvorgänge im DVM, Hannover, 6/7 October 1981
10 Dole, M. 'The Radiation Chemistry of Macromolecules', Academic Press, New York–London, 1973, 91
11 Ohnishi, S. and Nitta, I. *J. Polym. Sci.* 1959, **38**, 451
12 Benoit, M., Grubisic, Z. and Rempp, P. *J. Polym. Sci. B* 1967, **5**, 753
13 Charlesby, A. 'Atomic Radiation and Polymers', Pergamon Press, Oxford, 1960
14 Charlesby, A. *Radiat. Phys. Chem.* 1977, **10**, 177
15 Simitzis, V. J. *Atomkernenergie* 1979, **33**, 52 and references therein
16 Inokuti, M. *J. Chem. Phys.* 1960, **33**, 1607; *J. Chem. Phys.* 1963, **38**, 2999
17 Flory, P. J. 'Principles of Polymer Chemistry', Cornell University Press, Ithaca, N.Y., 1975
18 Kausch, H. H. 'Polymer Fracture', Springer-Verlag, Berlin–Heidelberg, 1978, 141
19 De Gennes, P. G. *C.R. Acad. Sc. Paris* 1980, **B291**, 219
20 Jelenic, J., Kirste, R. G., Schmitt, B. J. and Schmitt-Strecker, S. *Makromol. Chem.* 1979, **180**, 2057
21 Crank, J. 'Mathematics of Diffusion', Clarendon Press, Oxford, 1975

APPENDIX

Analytical expressions for $C_A(x,t)$ and $C_B(x,t)$ may be readily obtained if the diffusion of each layer is assumed to be independent.

The initial and boundary conditions for $C_{A_L}(x,t)$ are:

$$\begin{cases} C_{A_L}(x,0)=1 & -a\leqslant x\leqslant 0 \\ C_{A_L}(x,0)=0 & x<-a \quad x>0 \end{cases}$$

$$\begin{cases} C_{A_L}(x,\infty)=\dfrac{a}{2(a+b)} & -(a+b)\leqslant x\leqslant (a+b) \\ C_{A_L}(x,\infty)=0 & x<-(a+b) \quad x>(a+b) \end{cases}$$

Using the reflection concept[21], the concentration distribution function for $C_{A_L}(x,t)$ is given as follows:

$$C_{A_L}(x,t)=\sum_{n=-\infty}^{+\infty}\left\{erf\frac{(a+b)+4n(a+b)-x}{2\sqrt{D_B t}}+ erf\frac{(a+b)-4n(a+b)+x}{2\sqrt{D_A t}}-erf\frac{a+4n(a+b)-x}{2\sqrt{D_B t}} -erf\frac{a-4n(a+b)+x}{2\sqrt{D_B t}}\right\}$$

The series was found to converge for $n\geqslant 5$.

The boundary conditions for $C_{B_L}(x,t)$ were:

$$\begin{cases} C_{B_L}(x,t)=1 & -(a+b)\leqslant x\leqslant b \\ C_{B_L}(x,t)=0 & x<-(a+b) \quad x>-b \end{cases}$$

$$\begin{cases} C_{B_L}(x,\infty)=\dfrac{b}{2(a+b)} & -(a+b)\leqslant x\leqslant +(a+b) \\ C_{B_L}(x,\infty)=0 & x<-(a+b) \quad x>(a+b) \end{cases}$$

Using the same technique as that for $C_{A_L}(x,t)$, the distribution function for $C_{B_L}(x,t)$ is obtained:

$$C_{B_L}(x,t)=\sum_{n=-\infty}^{+\infty}\left\{erf\frac{a+4n(a+b)-x}{2\sqrt{D_B t}}+erf\frac{a-4n(a+b)+x}{2\sqrt{D_B t}}\right\}$$